Cardiovascular Research (2015) **108**, 197–208
doi:10.1093/cvr/cvv212

LKB1 deletion causes early changes in atrial channel expression and electrophysiology prior to atrial fibrillation

Grace E. Kim[1], Jenna L. Ross[2†], Chaoqin Xie[3], Kevin N. Su[1], Vlad G. Zaha[2], Xiaohong Wu[2], Monica Palmeri[2‡], Mohammed Ashraf[2¶], Joseph G. Akar[2], Kerry S. Russell[2§], Fadi G. Akar[3], and Lawrence H. Young[1,2*]

[1]Department of Cellular and Molecular Physiology, Yale University, New Haven, CT 06520, USA; [2]Yale Cardiovascular Research Center, Section of Cardiovascular Medicine, Department of Internal Medicine, Yale University School of Medicine, 333 Cedar Street, New Haven, CT 06520, USA; and [3]Cardiovascular Research Center, Mt. Sinai School of Medicine, New York, NY 10029, USA

Received 14 July 2014; revised 9 July 2015; accepted 14 July 2015

Time for primary review: 31 days

Aims Liver kinase B1 (LKB1) is a protein kinase that activates the metabolic regulator AMP-activated protein kinase (AMPK) and other related kinases. Deletion of LKB1 in mice leads to cardiomyopathy and atrial fibrillation (AF). However, the specific role of the LKB1 pathway in early atrial biology remains unknown. Thus, we investigated whether LKB1 deletion altered atrial channel expression and electrophysiological function in a cardiomyocyte-specific knockout mouse model.

Methods and results We performed a systematic comparison of αMHC-Cre LKB1$^{fl/fl}$ and littermate LKB1$^{fl/fl}$ male mice. This included analysis of gene expression, histology, and echocardiography, as well as cellular and tissue-level electrophysiology using patch-clamp recordings *in vitro*, optical mapping *ex vivo*, and ECG recordings *in vivo*. At postnatal day 1, atrial depolarization was prolonged, and Na_v1.5 and Cx40 expression were markedly down-regulated in MHC-Cre LKB1$^{fl/fl}$ mice. Inward sodium current density was significantly decreased in MHC-Cre LKB1$^{fl/fl}$ neonatal atrial myocytes. Subsequently, additional alterations in atrial channel expression, atrial fibrosis, and spontaneous onset of AF developed by 2 weeks of age. In adult mice, abnormalities of interatrial conduction and bi-atrial electrical coupling were observed, likely promoting the perpetuation of AF. Mice with AMPK-inactivated hearts demonstrated modest overlap in channel expression with MHC-Cre LKB1$^{fl/fl}$ hearts, but retained normal structure, electrophysiological function and contractility.

Conclusions Deletion of LKB1 causes early defects in atrial channel expression, action potential generation and conduction, which precede widespread atrial remodelling, fibrosis and AF. LKB1 is critical for normal atrial growth and electrophysiological function.

Keywords Atrial fibrillation • Cellular signalling pathways • LKB1

1. Introduction

The incidence of atrial fibrillation (AF) is rising worldwide,[1] linked in part to the increasing prevalence of metabolic disorders.[2] However, alterations in metabolism and metabolic signalling pathways that might be involved in AF development have not been studied.[3]

The liver kinase B1 (LKB1) is a serine/threonine kinase that activates 13 downstream kinases, including AMP-activated protein kinase

* Corresponding author. Tel: +1 203 785 4102; fax: +1 203 785 7567, E-mail: lawrence.young@yale.edu
† Present address. Division of Biomedical Sciences, Memorial University of Newfoundland, 300 Prince Philip Drive, St. John's, NL, Canada A1B 3V6.
‡ Present address. Maine Medical Center, 22 Bramhall St, Portland, ME 04102, USA.
¶ Present address. Department of Ophthalmology, Alexandria University Hospital, Alexandria 21526, Egypt.
§ Present address. Novartis Institutes for Biomedical Research, Novartis Institutes for BioMedical Research, Inc., USCA, 602-368F, 220 Massachusetts Avenue, Cambridge, MA 02139, USA.

(AMPK), which is a critical component of the metabolic stress response.[4] LKB1 is expressed in abundance in the liver, skeletal muscle, and heart in mice and humans.[5–7] Subcellular LKB1 localization and enzymatic activity are regulated by its interaction with MO25 and STRAD subunits in a heterotrimeric complex.[8,9] Disruption of this complex alters LKB1 activity, leading to human disease. Loss-of-function LKB1 mutations are found in lung adenocarcinomas[10] and in cancer-prone Peutz-Jeghers Syndrome patients.[11] The incidence of AF in Peutz-Jeghers Syndrome is unknown. However, a truncation mutation in the gene encoding STRAD, resulting in LKB1 inactivation,[12] has been found in children with severe seizures and atrial defects, and one was diagnosed with supraventricular tachycardia.[13]

Animal models suggest that LKB1 may have an important role in the heart. Mice with global deletion of LKB1 die embryonically due to vascular abnormalities,[14] whereas those with tissue-specific deletion often have postnatal abnormalities.[15] Conditional LKB1 deletion in striated muscle causes myopathy and enlarged atria.[6,16,17] Cardiomyocyte-specific LKB1 deletion leads to cardiac hypertrophy, left ventricular (LV) contractile dysfunction, AF, and premature death.[18]

We postulated that LKB1 might have a primary role in modulating electrical function in the heart and investigated the effects of cardiac-specific LKB1 deletion in a mouse model that spontaneously develops persistent AF. The aim of this study was to define whether LKB1 regulates early atrial channel expression, electrophysiology, growth, and function. To understand the potential contribution of loss of AMPK activity in this model, we performed parallel experiments in mice with genetic AMPK inactivation.

2. Methods

2.1 Animals

All procedures were approved by the Yale and Mt. Sinai IACUC committees, and conformed to the NIH guidelines. Cardiomyocyte-specific LKB1 knockout mice were generated by crossing LKB1$^{fl/fl}$ mice[19] with αMHC-Cre mice.[20] Mice were backcrossed for 10 generations into a C57BL/6 background. AMPK-inactivated or 'kinase-dead' (KD) C57BL/6 transgenic mice, expressing a catalytically inactive α2 subunit (rat K45R) in the heart,[21] were also studied. Littermate LKB1$^{fl/fl}$ and MHC-Cre LKB1$^{fl/fl}$ mice as well as wild-type and AMPK KD mice were compared.

2.2 Electrocardiography

Surface ECGs were performed under isoflurane anaesthesia (0.5–2%). Lead II signal was amplified (Animal Bio Amp and PowerLab 8/30) and analysed with LabChart (AD Instruments Colorado Springs, CO). Recordings were made after an initial stabilization period with heart rates 450–600 min^{-1}. A total of 8–10 rhythm strips, each consisting of five consecutive beats, were manually selected to calculate the average heart rate, P-wave duration, PR interval, and QRS duration. Ectopic beats were excluded from the analysis.

2.3 Echocardiography

Echocardiography was performed with isoflurane while maintaining body temperature. Cardiac morphology and function were examined by using a high-resolution ultrasound (VisualSonics, Toronto, ON). A total of six measurements were made in the short- and long-axis views. Atrial cross-sectional diameter was measured in the long-axis view, and LV size and function was assessed in the short-axis view, using 2D-guided M-mode imaging. Measurements from the six acquisitions were averaged.

2.4 Optical action potential mapping

High-resolution optical action potential (AP) mapping of superfused atrial preparations was performed as previously described.[22,23] Heart tissue preparations were stained with the voltage-sensitive dye, di-4-ANEPPS, for 5 min and continuously superfused with warmed oxygenated Tyrode solution containing (in mmol/L): 114 NaCl, 25 $NaHCO_3$, 4.6 KCl, 1.5 $CaCl_2$, 1.2 Na_2HPO_3, 0.7 $MgCl_2$, and 10 glucose. Preparations were maintained within a custom-designed, temperature-regulated imaging chamber, with the endocardial surface facing the imaging window in the presence of the electromechanical uncoupling agent blebbistatin (10 μM). The voltage-sensitive dye was excited with filtered light (515 ± 5 nm) from a quartz tungsten halogen lamp; the fluorescence was filtered (>620 nm) and directed onto a high-resolution CCD camera using an optical microscope. Preparations were paced from the right atrium at pacing cycle lengths ranging from 140 to 40 ms. Action potentials were recorded from 4 × 4 mm^2 regions of both the right and left atria.

2.5 Histology

Mice were heparinized (1000 U/kg) and anaesthetized with pentobarbital (60 mg/kg ip). The inferior vena cava was cut and the heart was perfused via the LV apex with cardioplegia solution containing (in mM): 10 HEPES, 150 KCl, and 5 EDTA, and fixed in paraformaldehyde. Fixed sections were stained as indicated by the Yale Mouse Research Pathology laboratory. Micrographs of samples were taken using the Eclipse 80i microscope (Nikon Instruments, Melville, NY).

2.6 Immunofluorescence

Deparaffinized and serially rehydrated tissue sections underwent heat-induced antigen retrieval in 1 mM Tris solution, pH 9.0. Sections were perforated in 0.3% Triton X-100 DPBS solution, and blocked with 10% normal goat serum before overnight incubation with: Cx40 (#Cx40-A; Alpha Diagnostic, San Antonio, TX) or Cx43 (#3512; Cell Signaling, Beverly, MA), as indicated, and αMHC (#ab15; Abcam, Cambridge, MA) to stain cardiomyocytes; nuclei were counterstained with DAPI. For TUNEL staining, sections were permeabilized with nuclease-free proteinase K (Roche, Indianapolis, IN) for 15 min at room temperature. Apoptotic cells were quantified after TUNEL staining with the *in situ* cell death detection kit (Roche), and DAPI nuclear staining, as reported previously.[24]

2.7 RT-qPCR

Total RNA was extracted using the NucleoSpin RNA XS kit (Macherey-Nagel, Bethlehem, PA). NanoDrop2000 (Thermo Fisher Scientific, Waltham, MA) was used to quantify and monitor RNA quality. Samples were reverse-transcribed using the SuperScript VILO kit (Invitrogen, Grand Island, NY). Target-specific primers were designed using Primer-BLAST (see Supplementary material online, *Table S1*). PCR was carried out with 5 μM of each primer and 1 ng of cDNA template with the SsoFastEvaGreen-Supermix (Bio-Rad, Hercules, CA), using a CFX96 C1000 Thermal Cycler (Bio-Rad). All data were normalized to ribosomal protein L32 (*Rpl32*), and expressed relative to control values.

2.8 Cell isolation and electrophysiology

Neonatal [postnatal day (PD)1–3] atrial myocytes were isolated from anaesthetized male (pentobarbital, 60 mg/kg ip) mice according to published methods.[25] Inward sodium current was measured at room temperature using the patch-clamp technique.[26] In brief, cells held at −80 mV were step depolarized from −90 to +45 mV in 5 mV steps of 20 ms in duration, with 60 ms interpulse intervals. Recording chamber solution contained (in mM) 25 NaCl, 132.5 CsCl, 1.8 $CaCl_2$, 1 $MgCl_2$, 0.1 $CdCl_2$, 5 HEPES, and 11 glucose, pH 7.4, with CsOH; pipette solution contained 5 NaCl, 135 CsF, 10 EGTA, 5 MgATP, and 5 HEPES, pH 7.2. As indicated, tetrodotoxin (TTX) was applied to the bath chamber at final concentration of 10 μM. Recordings were made using the ECP-9 Patch Clamp amplifier and the Pulse software (HEKA, Holliston, MA), and analysed using Igor Pro 6.3.

2.9 Western blot analysis

Rapidly frozen atrial and ventricular tissues were homogenized using the Ultra Turrax T8 disperser (IKA Wilmington, DE) in buffer containing (in mmol/L): 20 HEPES, 50 β-glycerol phosphate, 2 EGTA, 1 DTT, 10% glycerol, and 1% Triton X-100, supplemented with phosphatase and proteinase inhibitors.[21,27] Protein homogenates (15 μg for cytosolic and 45 μg for membrane proteins) were separated on precast gels, and transferred onto PVDF membranes. Membranes were blocked with 5% milk in TBST solution and incubated overnight with indicated primary antibody. The following antibodies were used: total-acetyl-CoA carboxylase (ACC; #3662), phospho-ACC Ser[79] (#3661), α-tubulin (#2125), Cx43 (#3512), Na/K ATPase (#3010), total-phospholamban (#8495; hitherto from Cell Signaling), $Na_v1.5$ (a gift from Dr Peter Mohler), Cx40 (#Cx40-A; Alpha Diagnostic), Cx45 (#40-7000; Invitrogen), phospho-phospholamban Ser[16]/Thr[17] (#ab62170; Abcam); and SERCA2 (#2A7-A1; Thermo Fisher Scientific). HRP-conjugated secondary antibodies were subsequently applied. Developed membranes were imaged using ChemiDoc XRS+ Imager (Bio-Rad). Densitometry values were determined using the ImageJ Software.

2.10 Statistical analysis

Data are presented as mean ± SEM. One-way ANOVA with Bonferroni's test, two-way ANOVA with the Sidak test, unpaired Student's *t*-test, or unpaired two-tailed Kolmogorov–Smirnov test analyses were performed using the Prism 6 Software (Graph Pad, La Jolla, CA). A value of $P < 0.05$ was considered statistically significant.

3. Results

3.1 Atrial conduction abnormalities and AF in MHC-Cre LKB1$^{fl/fl}$ mice

AF has been reported in one[18] but not in other[6,17,28] LKB1 deletion mouse models. To study the potential effects of LKB1 deletion on early

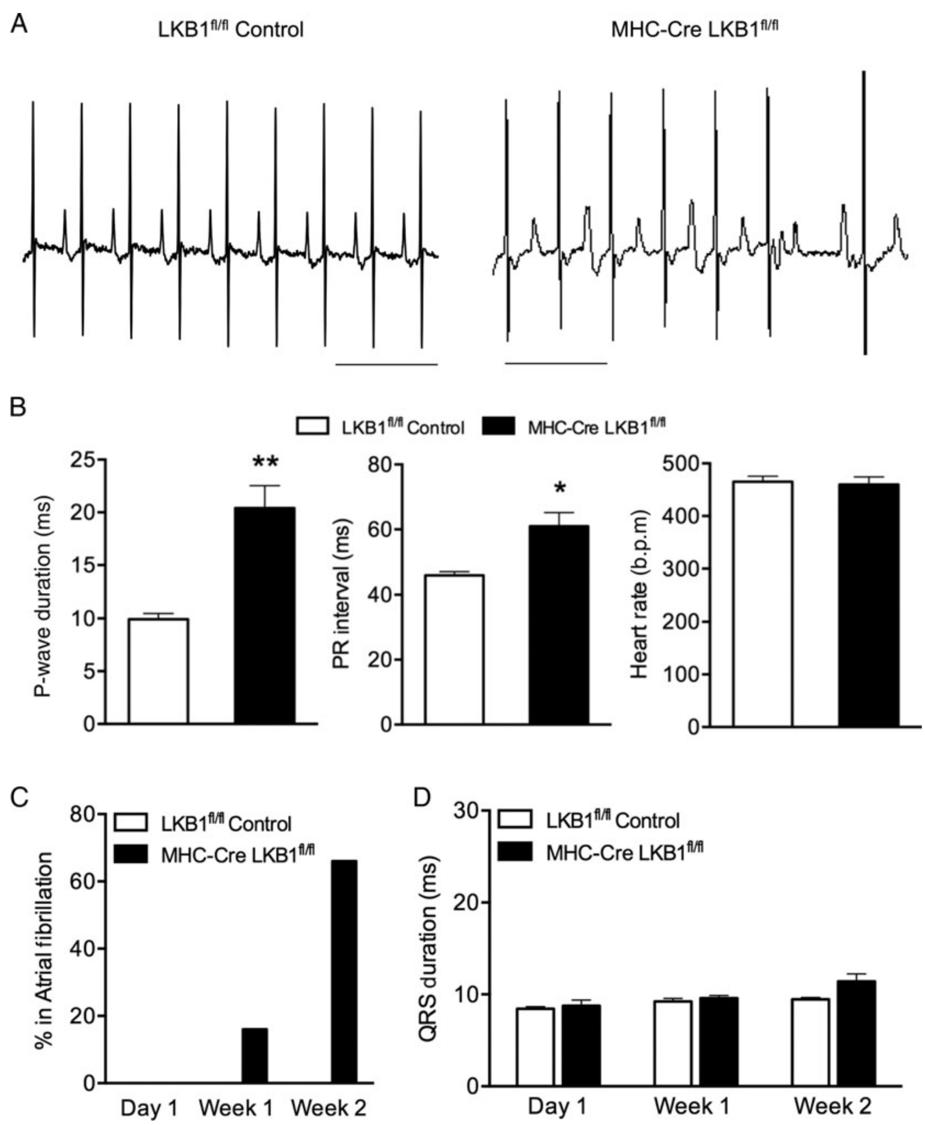

Figure 1 Cardiac LKB1 deletion results in early atrial conduction abnormalities and AF development. Cardiac rhythm and conduction were assessed at Day 1, Week 1, and Week 2. (*A*) Representative ECG lead II traces from mice at Day 1. Scale bars represent 200 ms. (*B*) Mean values for P-wave duration, PR interval, and heart rate in mice, at Day 1. (*C*) The percentage of mice that developed AF in the first 2 weeks of life. (*D*) QRS duration at each time point. $*P < 0.01$, $**P < 0.001$ vs. age-matched control group, $n = 5–9$, two-tailed Student's *t*-test.

cardiac conduction, we examined MHC-Cre LKB1$^{fl/fl}$ mice in their first 2 weeks of life using surface ECG monitoring. We observed frequent atrial ectopic complexes (*Figure 1A*), and a two-fold increase in P-wave duration in MHC-Cre LKB1$^{fl/fl}$ mice, suggestive of atrial conduction slowing (*Figure 1B*), as early as PD1. PR intervals were also prolonged, but heart rates were normal (*Figure 1B*). A majority of MHC-Cre LKB1$^{fl/fl}$ mice developed persistent AF spontaneously by Week 2 (*Figure 1C*). Both the efficiency of LKB1 deletion and concomitant inactivation of the downstream AMPK pathway were comparable in the atria and ventricles of the MHC-Cre LKB1$^{fl/fl}$ mouse hearts (see Supplementary material online, *Figure S1A* and *B*). In contrast to the atrial conduction abnormalities, ventricular conduction indexed by QRS duration remained unchanged in MHC-Cre LKB1$^{fl/fl}$ mice (*Figure 1D*), and we did not observe ventricular ectopy.

3.2 Postnatal atrial remodelling in LKB1 deletion mice

AF can be triggered by primary electrophysiological abnormalities that alter automaticity, conduction velocity, or repolarization in atrial cardiomyocytes.[29] However, AF can also result from conduction delay that is associated with atrial remodelling and fibrosis. Thus, we examined the timing of atrial remodelling, in order to determine the relationship between conduction abnormalities and structural changes in the MHC-Cre LKB1$^{fl/fl}$ mice. Atrial weights were normal at PD1, but subsequently were two-fold greater at Week 1 in MHC-Cre LKB1$^{fl/fl}$ mice compared with controls (*Figure 2A*). Interestingly, ventricular weights were unchanged at PD1 and slightly decreased at Week 2 in the knockout mice (*Figure 2A*). Body weights remained comparable (not shown).

We also examined heart histology at embryonic day (ED) 15.5, PD1, and Week 2 to delineate the timing of cellular remodelling associated with LKB1 deletion. Acute activation of the downstream AMPK pathway has an anti-hypertrophic effect in cultured rat neonatal ventricular cardiomyocytes,[18] but we found that LKB1 deletion did not affect atrial or ventricular myocyte cross-sectional areas at Week 2 (*Figure 2B*). Trichrome staining showed no evidence of extracellular fibrosis in the atria either at ED15.5 or PD1 (Day 1). Furthermore, ED15.5 hearts stained with picrosirius red, a more sensitive marker of collagen fibres,[30] showed no change in fibre density in the atria (see Supplementary material online, *Figure S2*). Subsequently, atrial but not ventricular fibrosis developed at Week 2 in MHC-Cre LKB1$^{fl/fl}$ mice (*Figure 2C*).

To identify potential mechanisms responsible for atrial remodelling, we analysed apoptosis by TUNEL staining, and gene transcripts for pro-fibrotic factors and inflammatory markers. Increased atrial fibrosis was not associated with atrial apoptosis, but there was a six-fold increase in ventricular apoptosis in the MHC-Cre LKB1$^{fl/fl}$ mice at PD1 (see Supplementary material online, *Figure S3A–C*). We found no histologic evidence of atrial inflammation, and CD34 transcripts were unchanged at Day 1 and actually reduced at Week 2 in MHC-Cre LKB1$^{fl/fl}$ mice (*Figure 2D*). In contrast, there was an increase in connective tissue growth factor (*CTGF*), endothelin-1 (*Edn1*), and collagen 1A (*Col1a1)* transcripts at Week 2, indicating initiation of pro-fibrotic signalling as early as Day 1 despite the absence of histological abnormalities (*Figure 2D*).

3.3 Atrial-specific changes in ion channel expression

Since P-wave prolongation at Day 1 appeared to occur in the absence of structural remodelling, we hypothesized that early atrial-specific electrical remodelling might be a direct consequence of LKB1 deletion. Thus, we examined the expression levels of key ion channels, transporters, and gap junction proteins at this time point. Consistent with their prolonged intra-atrial conduction, MHC-Cre LKB1$^{fl/fl}$ mice had significantly reduced atrial Cx40 (*Gja5*) and $Na_v1.5$ (*Scn5a*) transcripts at Day 1 (*Figure 3A*). Atrial Cx43 (*Gja1*) and Cx45 (*Gjc1*) were also decreased early, showing significant changes by Week 2 (*Figure 3*), with parallel decreases in protein expression evident on immunoblots of atrial homogenates (see Supplementary material online, *Figure S5*). These changes were also reflected in reduced atrial cardiomyocyte Cx40 and Cx43 IF staining in heart sections, both at Day 1 (*Figure 3B*) and ED15.5 (see Supplementary material online, *Figure S4*).

To assess the functional consequences of decreased atrial $Na_v1.5$ expression at Day 1 (*Figure 4A*), we measured the density of the inward current in isolated neonatal atrial cardiomyocytes. This inward current was completely suppressed by the sodium channel blocker TTX, confirming that it was due to sodium ion flux (see Supplementary material online, *Figure 6A* and *B*). Our recordings showed that the inward sodium current (I_{Na}) was diminished in MHC-Cre LKB1$^{fl/fl}$ myocytes compared with control (*Figure 4B* and *C*). There was a 60% reduction in peak I_{Na} density at -15 mV in myocytes isolated from MHC-Cre LKB1$^{fl/fl}$ compared with those from control atria (*Figure 4D*). No differences in cell capacitance or inactivation tau kinetics were found (see Supplementary material online, *Figure S6D*). Taken together, these findings demonstrate that LKB1 deletion significantly impairs cardiomyocyte excitability by reducing Nav1.5 expression, prior to structural remodelling in the atria.

Additional early decreases in atrial transcript expression included the sarcolemmal voltage-dependent calcium channel $Ca_v3.2$ (*Cacna1h*), delayed rectifier potassium channel $K_v7.1$ (*Kcnq1*), pore-forming subunit of the K_{ATP} (*Kcnj8*) channel, the inwardly rectifying Kir2.4 (*Kcnj14*), and TASK-1 (*Kcnk3*) channels (see Supplementary material online, *Figure S7A* and *B*).

3.4 Late atrial electrophysiological abnormalities of the MHC-Cre LKB1$^{fl/fl}$ mice

Consistent with a prior report,[18] MHC-Cre LKB1$^{fl/fl}$ mice had a shorter lifespan, with death occurring as early as 13 weeks of age (see Supplementary material online, *Figure S8*). Thus, we elected to study the late electrophysiological function in MHC-Cre LKB1$^{fl/fl}$ mice between 10 and 12 weeks of age. We performed high-resolution optical AP imaging in superfused bi-atrial preparations (atrial mapping) and Langendorff-perfused hearts (ventricular mapping). Atrial AP duration (APD) was prolonged by two-fold in MHC-Cre LKB1$^{fl/fl}$ mice compared with controls (*Figure 5A* and see Supplementary material online, *Figure 9A*). This finding may reflect the down-regulation of K^+ channel expression that we observed. While atrial preparations from control mice could be paced at cycle lengths down to 50 ms, MHC-Cre LKB1$^{fl/fl}$ mice exhibited early loss of excitability at cycle lengths $<$80 ms (*Figure 5A*). These data are consistent with a reduced depolarization reserve in MHC-Cre LKB1$^{fl/fl}$ mice possibly due to lower $Na_v1.5$ levels. Furthermore, rapid pacing of atrial preparations from MHC-Cre LKB1$^{fl/fl}$ mice resulted in a 2 : 1 pattern of conduction block (see Supplementary material online, *Figure S9B–D*), revealing a rate dependence of conduction. Additionally, quantification of the normalized atrial AP upstroke velocity, an index of atrial excitability, was significantly reduced in MHC-Cre LKB1$^{fl/fl}$ mice (*Figure 5B*).

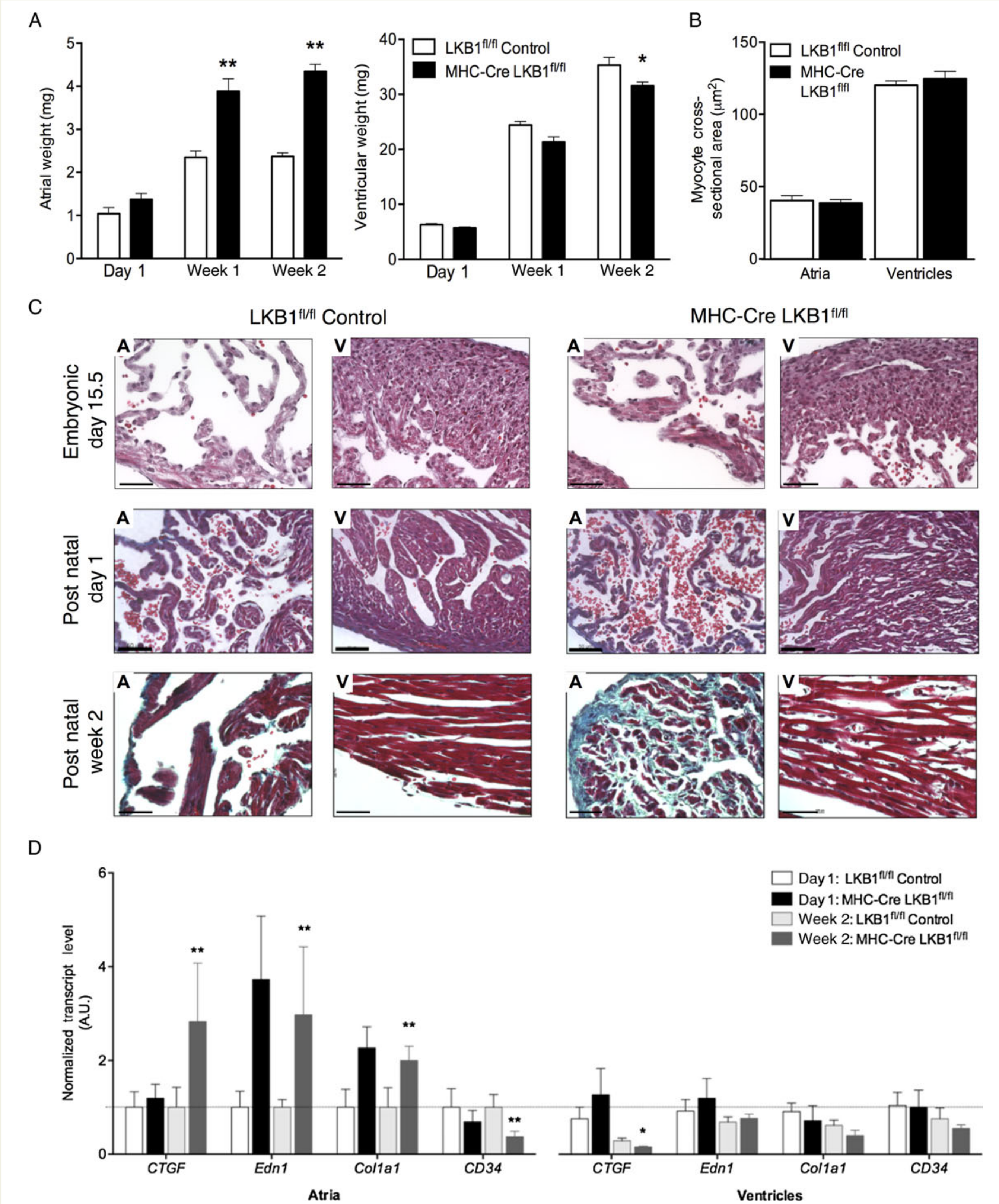

Figure 2 Cardiac LKB1 deletion leads to differential atrial and ventricular remodelling during early growth. (*A*) Atrial and ventricular mass for MHC-Cre LKB1$^{fl/fl}$ and LKB1$^{fl/fl}$ mice. $*P < 0.01$, $**P < 0.001$ vs. age-matched control, $n = 5-14$, one-way ANOVA. Whole-heart sections were examined at ED 15.5, PD1, and Week 2. (*B*) Averaged myocyte cross-sectional area at Week 2. (*C*) Representative images of trichrome-stained left atria ("A") and left ventricle ("V") at the indicated time points. Scale bars represent 50 µm. (*D*) Chamber-specific transcript levels of connective tissue growth factor (*CTGF*), endothelin-1 (*Edn1*), collagen-1 (*Col1a1*), and CD34 (*CD34*) on Day 1 and Week 2. $*P < 0.05$, $**P < 0.01$ vs. age-matched control group, $n = 6$, two-tailed Student's *t*-test.

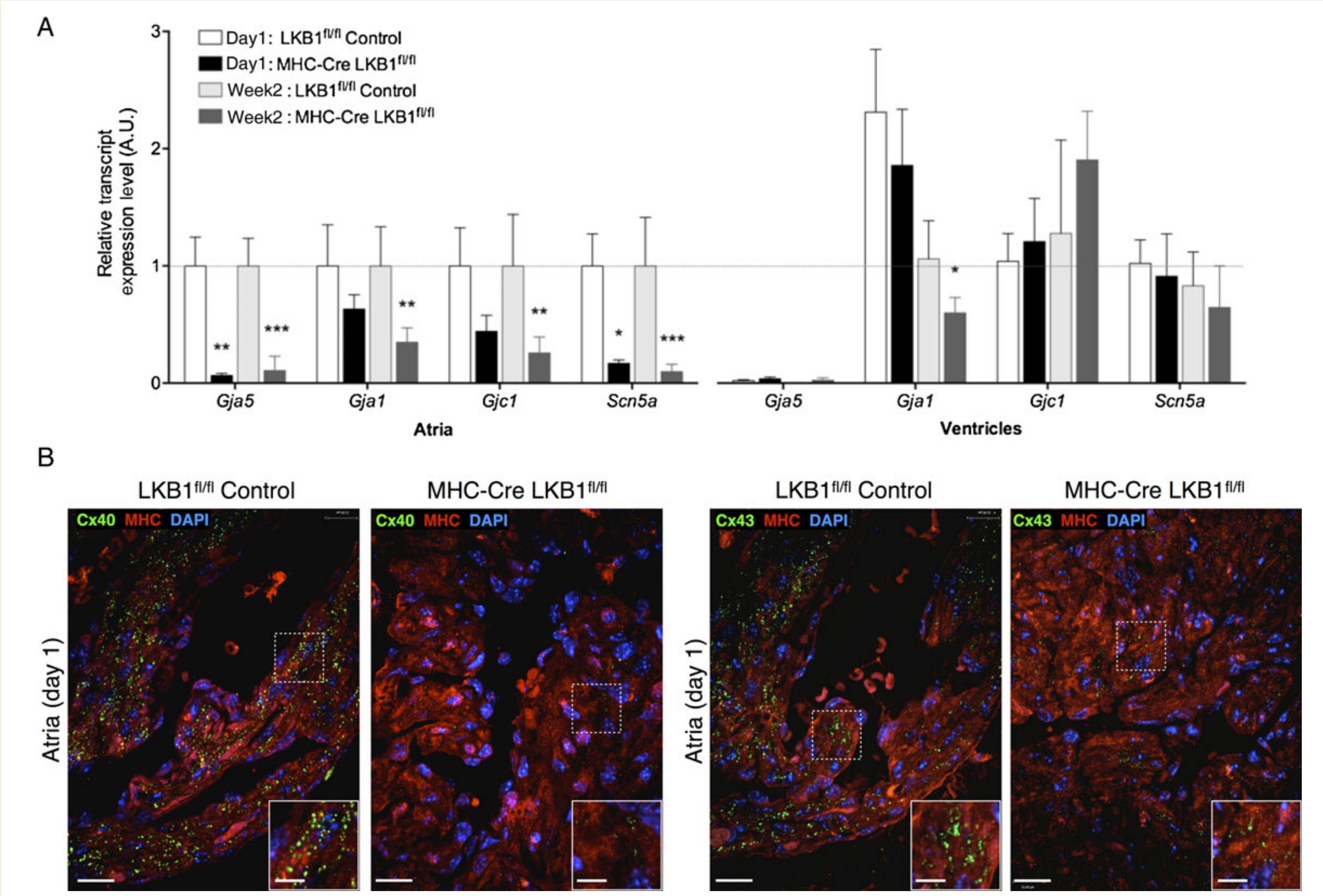

Figure 3 Cardiac LKB1 deletion leads to down-regulation of ion channels. Transcript levels of (*A*) gap junction proteins (*Gja5, Gja1, and Gjc1*) and the voltage-dependent sodium channel (*Scn5a*) were compared in the atria and ventricles at Day 1 and Week 2. $*P < 0.05$, $**P < 0.01$, $***P < 0.001$ vs. age-matched control group, $n = 6$, unpaired Student's *t*-test. (*B*) Representative IF images of Day 1 atrial sections, stained for Cx40 (left) or Cx43 (right), both labelled with green fluorophores. Scale bars represent 12 μm. (Insets) Zoom-in images of areas of interest indicated by dotted squares. Scale bars represent 6 μm.

Delayed inter-atrial electrical coupling is associated with arrhythmogenesis.[31] We therefore investigated whether inter-atrial electrical coupling was delayed in the adult MHC-Cre LKB1$^{fl/fl}$ mice. The right atrium was paced, while we measured the right and left atrial AP responses (*Figure 5C*). Whereas pacing elicited AP responses in both atria in controls, AP responses were confined to the right atrium in MHC-Cre LKB1$^{fl/fl}$ preparations, indicating a complete loss of inter-atrial electrical coupling.

Compared with these marked alterations in the atria, changes in ventricular electrophysiology were modest. A trend towards longer APDs was found in MHC-Cre LKB1$^{fl/fl}$ ventricles over a range of cycle lengths. Differences, reaching a maximum of 1.2-fold increase, only reached statistical significance at relatively long (i.e. 140 ms) pacing cycle lengths (*Figure 6A*). Despite these alterations, conduction velocity remained unchanged in MHC-Cre LKB1$^{fl/fl}$ ventricles vs. controls (*Figure 6B* and *C*). Collectively, these *ex vivo* data reveal pronounced electrophysiological dysfunction in the atria that may provide a suitable electrophysiological substrate to support the maintenance of AF *in vivo* in MHC-Cre LKB1$^{fl/fl}$ mice.

3.5 Effects of inactivation of AMPK signalling on early heart growth and electrophysiology

LKB1 is upstream of the metabolic fuel gauge/stress kinase AMPK, which also regulates the activity of selected ion channels,[32] cellular growth, and polarity.[33] Thus, we considered the role of AMPK in mediating the effects of LKB1 deletion, and performed parallel studies to determine whether AMPK-inactivated 'KD' mice[21] shared similar abnormalities. At Week 2, ECG recordings were normal in KD mice (see Supplementary material online, *Figure S10A* and *B*). Size and weight of the hearts were also normal (not shown). At the molecular level, KD mice exhibited decreased atrial *Scn5a* and increased *Col1a1* transcripts, but no alterations in gap junction proteins (see Supplementary material online, *Figure S10C*). Thus, the limited changes present in the KD atria were insufficient to induce the electrophysiological abnormalities or structural remodelling seen in MHC-Cre LKB1$^{fl/fl}$ mice.

We determined the degree of AMPK inactivation by assessing phosphorylation of downstream ACC in the two models. ACC

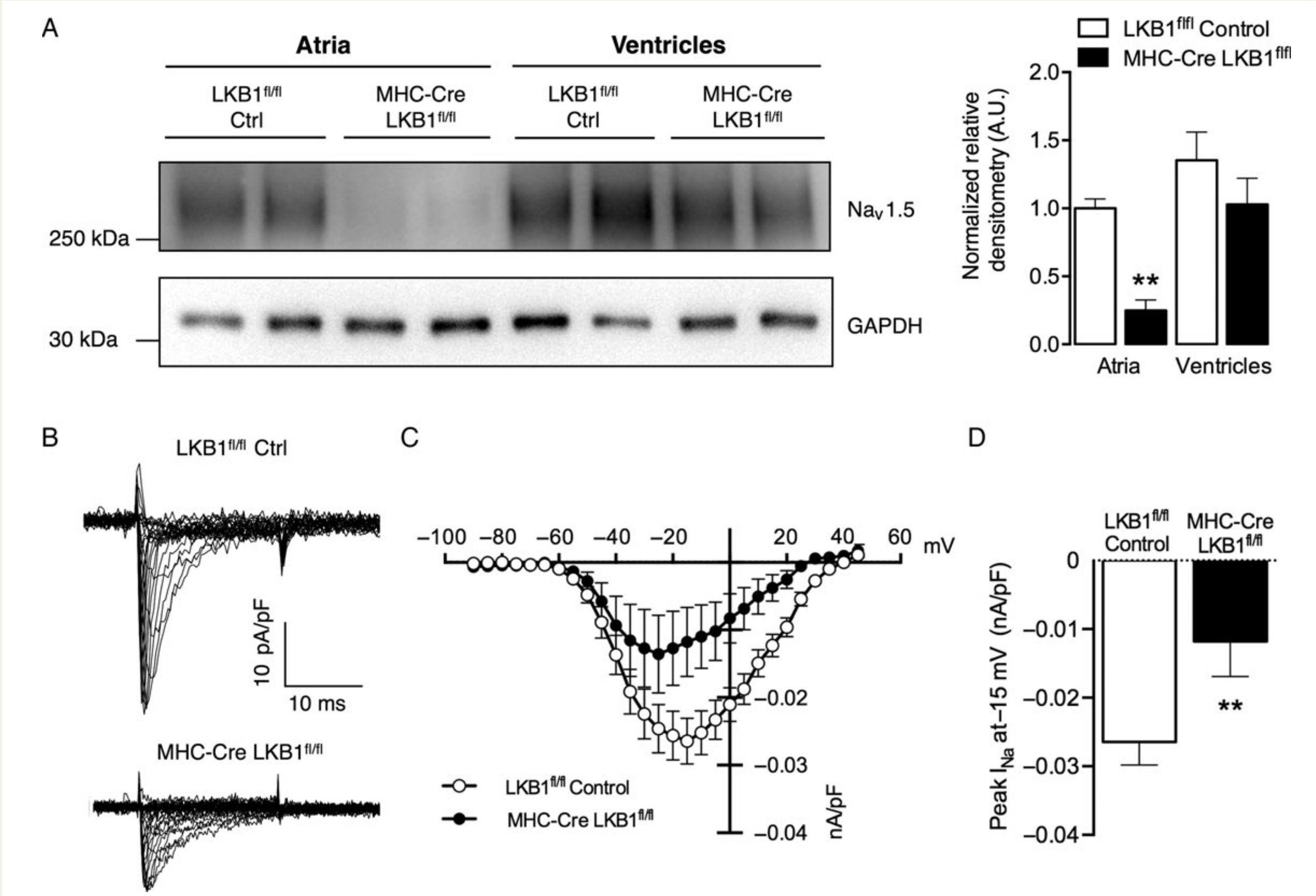

Figure 4 Cardiac LKB1 deletion leads to decreased sodium channel $Na_v1.5$ expression and function in the atria. (*A*) A representative immunoblot for $Na_v1.5$ in 1-day-old heart homogenates with quantification by densitometry in bar graph to the right. (*B*) Representative traces of whole-cell patch-clamp measurements of inward sodium current density in MHC-Cre LKB1$^{fl/fl}$ and LKB1$^{fl/fl}$ neonatal atrial cardiomyocytes. (*C*) I-V plot of inward sodium current density in MHC-Cre LKB1$^{fl/fl}$ and LKB1$^{fl/fl}$ neonatal atrial cardiomyocytes. (*D*) The peak current amplitude at −15 mV was significantly lower in MHC-Cre LKB1$^{fl/fl}$ vs. LKB1$^{fl/fl}$ myocytes (**$P = 0.01$, unpaired two-tailed Kolmogorov–Smirnov test, $n = 14$–17 cells from 6–8 animals per group).

phosphorylation was decreased in both models, but more so in the MHC-Cre LKB1$^{fl/fl}$ compared with KD mice (see Supplementary material online, *Figure S10D*). As such, we could not exclude the possibility that greater inactivation of AMPK signalling contributed to the more prominent alterations in the MHC-Cre LKB1$^{fl/fl}$ mice.

Finally, we compared the effects of LKB1 deletion vs. AMPK inactivation on cardiac function in adult mice at 12 weeks. All MHC-Cre LKB1$^{fl/fl}$, but none of the KD mice, were in AF (*Figure 7A*). Echocardiograms showed LA enlargement, increased LV wall thickness, and diminished ejection fraction in LKB1 knockouts, but again not in KD mice (*Figure 7B*). Similarly, we found pronounced atrial fibrosis and myocyte hypertrophy only in MHC-Cre LKB1$^{fl/fl}$ mice (*Figure 7C* and see Supplementary material online, *Figure S11*). Taken together, these results demonstrate substantially more pronounced cardiac remodelling and electrophysiological abnormalities in fully backcrossed syngeneic adult mice with LKB1 deletion compared with those with AMPK inactivation.

4. Discussion

These findings support an important role for LKB1 signalling in atrial biology, demonstrating early electrophysiological abnormalities and subsequent structural remodelling in mice with LKB1 deletion in cardiac myocytes. LKB1 deletion resulted in decreased expression and function of ion channel and gap junction proteins that are critical to atrial excitability, intra-atrial conduction, and coupling. These changes started to develop prior to atrial structural remodelling and the onset of AF. However, LKB1 deletion subsequently led to atrial enlargement and fibrosis, without evidence of necrosis, inflammation, apoptosis, or cardiomyocyte hypertrophy. The remodelling and fibrosis led to marked electrophysiological abnormalities in adult mice that very likely contributed to the perpetuation of AF.

4.1 Changes in ion channel expression and function in MHC-Cre LKB1$^{fl/fl}$ mice

These results indicate that LKB1 has a critical early atrial-specific role, modulating the expression of ion channels and gap junction proteins that underlie the generation and propagation of the AP. During late embryonic development, there was a significant decrease in the expression of Cx40, the atrial-enriched connexin isoform that facilitates AP propagation.[34,35] LKB1 deletion also led to marked down-regulation of neonatal atrial $Na_v1.5$ expression and a decrease in inward sodium current in isolated atrial cardiomyocytes. The combined alterations in

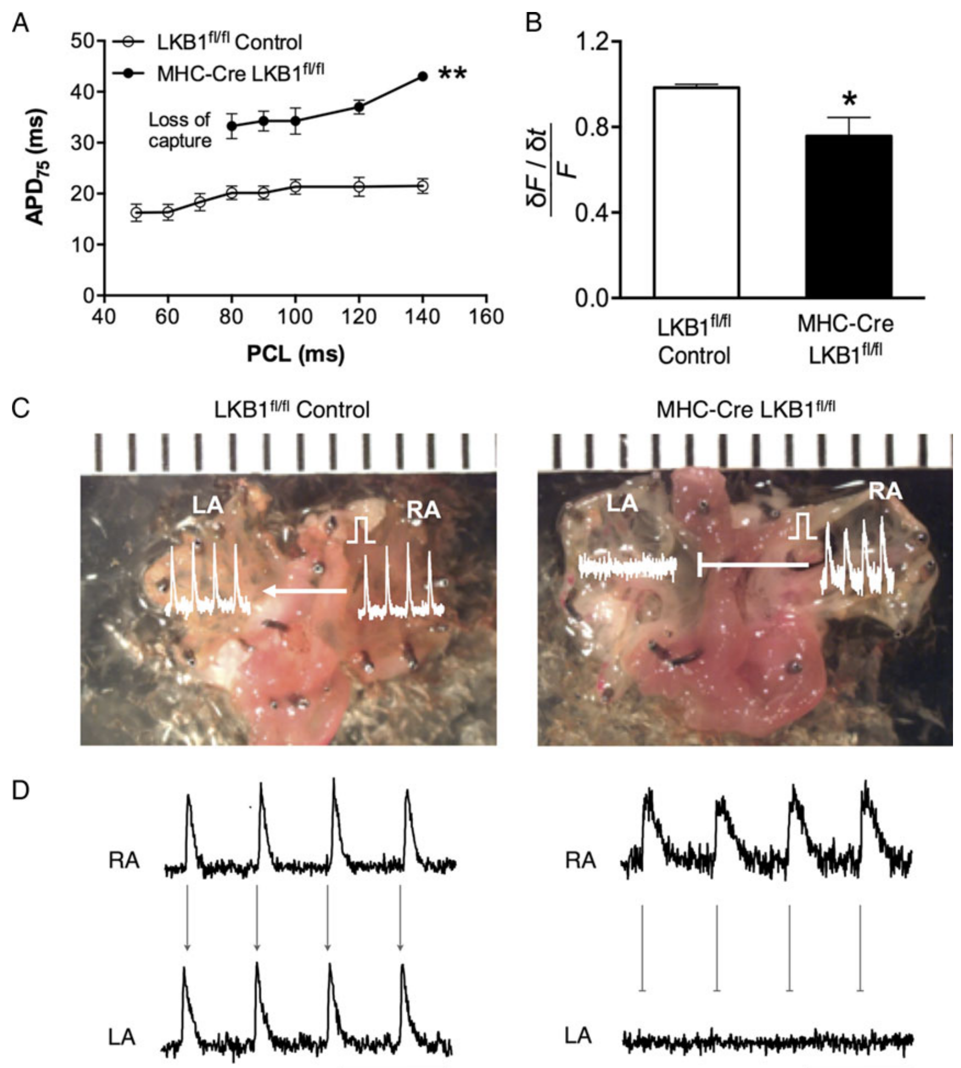

Figure 5 Cardiac LKB1 deletion results in atrial APD prolongation and uncoupled intra-atrial conduction. Isolated atria loaded with the voltage-sensitive dye, di-4-ANEPPS, were paced from the right atrium (RA) at pacing cycle lengths (PCL) from 40 to 140 ms. (*A*) APD at 75% repolarization plotted against PCL. $^{**}P < 0.001$ vs. control, $n = 4–6$, two-way ANOVA with the Sidak multiple comparison test. (*B*) Upstroke velocity change in the two groups is compared. $^{*}P < 0.01$ vs. control group, $n = 4–6$, unpaired Student's *t*-test. (*C*) Photos of the experimental setup showing both atria, as well as the RA pacing sites. (*D*) Representative AP traces reveal intra-atrial uncoupling in the MHC-Cre LKB1$^{fl/fl}$ preparation. Scale bars represent 200 μm.

Cx40 and $Na_v1.5$ could account for the prolonged P-wave duration, indicative of an intra-atrial conduction delay, observed at PD1.

Studies on Cx40- or $Na_v1.5$-ablated mouse models provide an additional perspective on our findings. In mice, Cx40 deletion leads to multiple conduction abnormalities, including atrioventricular block and atrial re-entrant tachycardia.[36,37] Heterozygous $Na_v1.5$ deletion slows sino-atrial, atrioventricular, and intra-ventricular conduction pathways in mice.[38,39] Although deletion of either protein alone does not cause AF in mice *per se*, reduced expression of either $Na_v1.5$ or Cx43 heightens the susceptibility to AF in response to stressors.[38,40] Furthermore, a concomitant decrease in $Na_v1.5$ and Cx43 expression increases vulnerability to ventricular arrhythmias in mice.[41] These studies suggest that the combined down-regulation of atrial $Na_v1.5$ and connexin expression could be central to AF development in the MHC-Cre LKB1$^{fl/fl}$ mice. As alterations in potassium and calcium channels can also trigger AF,[42] it is possible that changes in the expression of these channels could also have contributed to their developing AF.

Hitherto unexplored in the previously reported LKB1 deletion mouse models,[18,28,43] our molecular and cellular studies indicate a novel role for LKB1 in the neonatal atria. Cardiomyocyte hypertrophy and fibrosis,[18] as well as increased inflammation and ROS generation,[43] have been proposed as precipitants of AF in mice with cardiac LKB1 deletion. These prior studies were performed in older mice (4–12 weeks age range) that had undergone substantial atrial remodelling. Our findings expand upon these previous observations by elucidating the early physiological and molecular abnormalities in MHC-Cre LKB1$^{fl/fl}$ mice. Early changes in channel expression occurred in the atria prior to the onset of AF. Thus, our results suggest that initial electrical remodelling may have an important role in their predisposition to the development of AF.

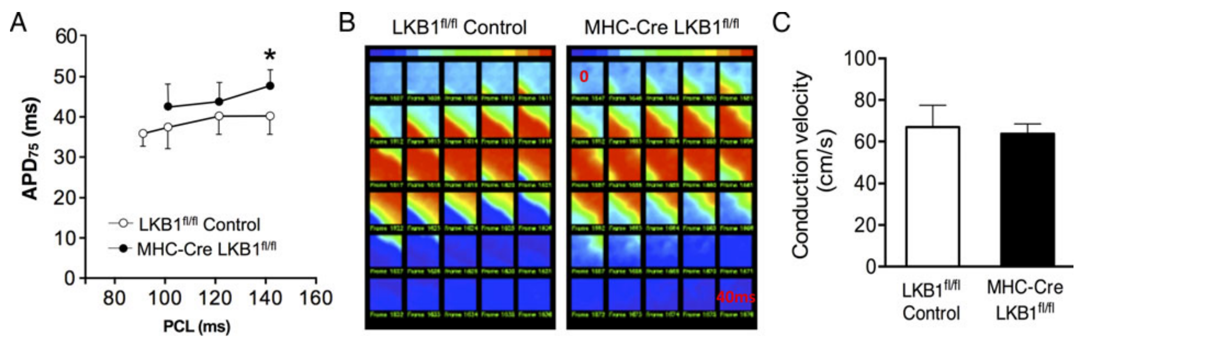

Figure 6 Effects of cardiac LKB1 deletion on ventricular electrophysiological function. Langendorff-perfused ventricles, isolated from control or LKB1-deleted mice at 10–12 weeks of age, were paced at various PCL. (*A*) APD at 75% repolarization plotted against PCL (*$P < 0.001$ against control, $n = 4$–6, two-way ANOVA with the Sidak multiple comparison test). (*B*) A representative pseudo-coloured map of the left ventricle, showing changes in di-4-ANEPPS fluorescence over time. (*C*) A plot comparing averaged conduction velocity.

4.2 Structural remodelling in MHC-Cre LKB1$^{fl/fl}$ mice

In adult mice, we found that cardiac LKB1 deletion caused substantial atrial fibrosis and remodelling, as has been seen in prior models with cardiac[29,43] and striated muscle[6] LKB1 deletion. Atrial fibrosis causes conduction slowing, wave break formation, and re-entrant excitation; thereby predisposing to AF.[44] Indeed, we observed pronounced electrophysiological abnormalities in atria from older mice with LKB1 deletion, using optical mapping techniques, that in part reflect the presence of atrial fibrosis and would favour the persistence of AF. Whether these intra-atrial conduction abnormalities further contribute to atrial contractile dysfunction and secondary structural remodelling is also possible and warrants further investigation.

Our studies show striking chamber-specific differences in MHC-Cre LKB1$^{fl/fl}$ mice, including greater fibrosis in the atria compared with the ventricles. These findings are reminiscent of results in mice expressing a constitutively activated TGF-β1 transgene in cardiomyocytes.[45] The predilection to fibrosis was postulated to reflect a greater sensitivity of atrial cardiomyocytes and/or fibroblasts to TGF-β1 or its downstream cytokines, such as CTGF secreted into the extracellular matrix.[45] Our MHC-Cre LKB1$^{fl/fl}$ mice demonstrated increased CTGF and endothelin-1 selectively in the atria, consistent with a role of LKB1 in modulating atrial pro-fibrotic pathways. Greater atrial fibrosis is not restricted to mouse models and has also been reported in the canine model of rapid ventricular pacing-induced dilated cardiomyopathy.[46] Elucidation of the mechanism responsible for this differential fibrotic reaction would be of interest and will require an additional study.

4.3 Role of LKB1-AMPK signalling in atrial growth and electrophysiology

AMPK-inactivated KD mice did not display the atrial electrophysiological alterations that were observed in MHC-Cre LKB1$^{fl/fl}$ mice. However, AMPK KD and MHC-Cre LKB1$^{fl/fl}$ mice had some overlapping changes in gene expression, including decreased $Na_v1.5$, suggesting that a subset of the observed effects of LKB1 deletion may be AMPK-dependent. It is possible that a lesser degree of AMPK pathway inactivation in KD, compared with MHC-Cre LKB1$^{fl/fl}$ mice, could explain the lack of electrophysiological and structural remodelling in the KD mice. This hypothesis would be consistent with the recent observation that striated muscle-specific AMPK β1β2 double knockout mice, which completely lack cardiomyocyte AMPK activity, develop cardiomyopathy, enlarged atria, and AF.[47] The precise role of loss of atrial AMPK activation in the development of AF in this model is unclear, since ECGs were assessed only in adult mice after the onset of LV contractile dysfunction, heart failure, and atrial remodelling. LKB1 also modulates the activity of 12 other LKB1 substrates, termed AMPK-related kinases (ARKs), whose actions are poorly understood in the heart.[5] The lack of activation of one or more ARKs could also contribute to the atrial phenotype that we observed and future studies will be needed to delineate the more specific roles of the ARKs and AMPK in atrial biology.

4.4 Clinical implications

LKB1 and AMPK are highly expressed in the human heart,[7,48] but their contribution to the development of clinical AF is uncertain. Inactivating mutations in LKB1 are found in Peutz-Jeghers Syndrome, which is characterized primarily by gastrointestinal polyposis and a high predisposition to malignancy,[19] but the incidence of atrial arrhythmias in these patients is unknown. Activating mutations in *PRKAG2*, which encodes the AMPK regulatory gamma 2 subunit, cause cardiomyopathy, Wolff-Parkinson-White syndrome, and atrial arrhythmias.[49] However, this phenotype is caused primarily by cardiomyocyte glycogen overload resulting from increased glucose uptake and glycogen synthesis.[50] Whether *PRKAG2* mutations also directly affect the expression or activity of atrial ion channels is not known.

Our finding that LKB1 deletion leads to spontaneous AF and a marked down-regulation of Cx40 and $Na_v1.5$ in the mouse has further potential clinical implications. In humans, decreased Cx40 expression due to a single nucleotide polymorphism (SNP) variant in the Cx40 (*GJA5*) gene promoter is associated with early onset AF.[51] The relationship of alterations in $Na_v1.5$ to human AF is less clear. A small cohort study of patients with valvular AF did not display decreased expression of *SCN5A* in surgically excised right atrial appendage samples.[42] However, a common SNP variant in *SCN5A*, as well as both loss- and gain-of-function mutations, have been identified in patients with AF.[52–54] Collectively, these findings demonstrate the importance of understanding how LKB1 downstream pathways regulate these channels in humans.

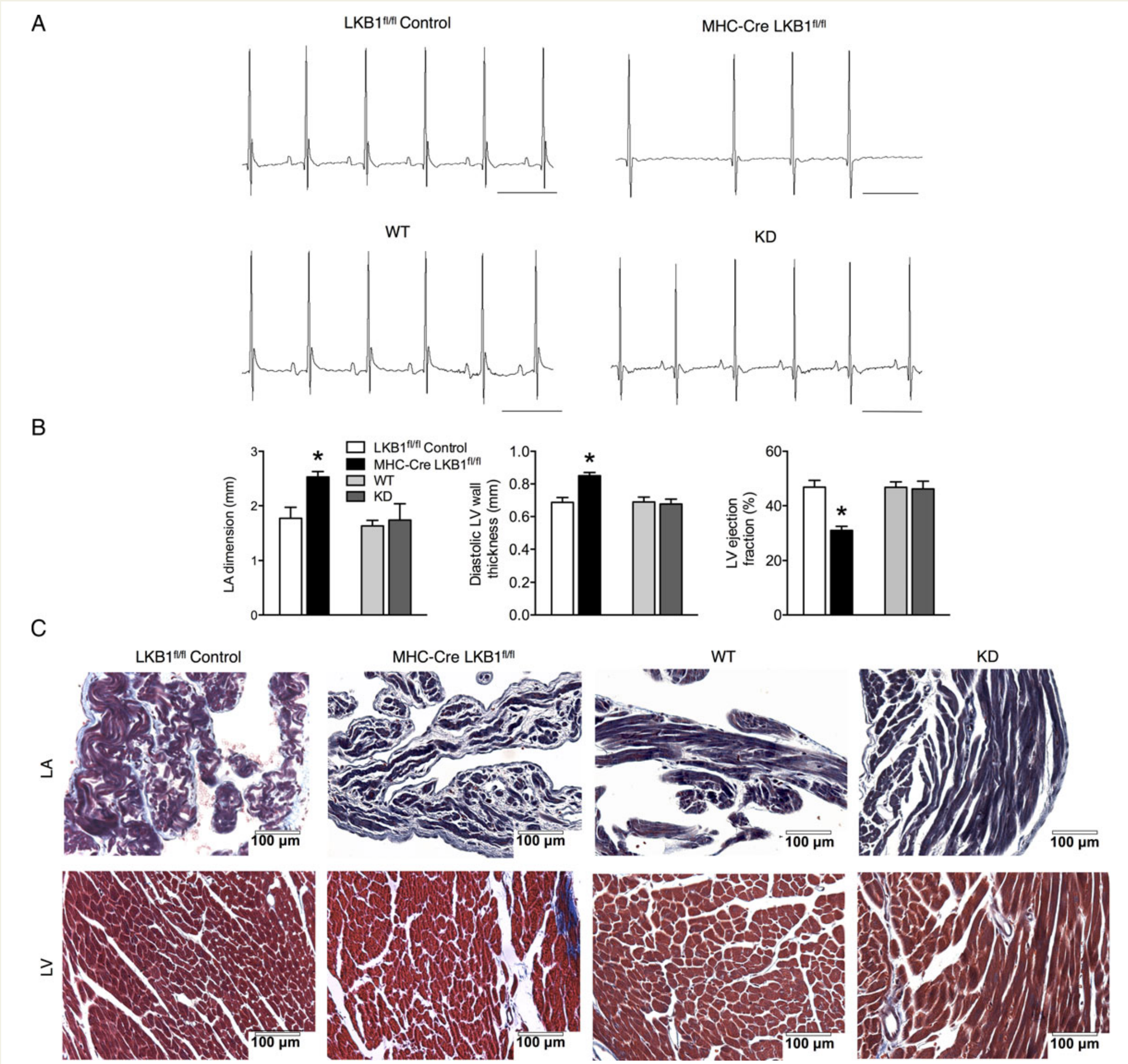

Figure 7 Differential effects of LKB1 deletion and AMPK inactivation on cardiac structure, function, and electrophysiology. MHC-Cre LKB1$^{fl/fl}$ and AMPK KD adult mice and their littermate controls were examined at 10 weeks of age. (*A*) Representative surface ECGs, demonstrating AF in LKB1-deleted mice ($n = 7-11$). Scale bars represent 125 ms. (*B*) Average atrial dimension, LV diastolic wall thickness, and ejection fraction (% EF) are plotted. $^*P < 0.05$ vs. control group, $n = 5-9$, two-way ANOVA. (*C*) Representative trichrome-stained images from whole-heart sections of 10-week-old MHC-Cre LKB1$^{fl/fl}$, KD, and their respective controls are shown.

5. Conclusions

In summary, LKB1 appears to play a critical role in normal atrial growth and electrophysiology in mice. Its deletion induces early atrial-specific reprogramming of ion channel and connexin expression, which give rise to electrophysiological abnormalities, prior to the onset of AF. These findings provide mechanistic insights into the predisposition to spontaneous AF caused by LKB1 deletion. Additional work is needed to elucidate the role of LKB1 and its downstream signalling pathways in the prevention or treatment of AF.

Supplementary material

Supplementary material is available at *Cardiovascular Research* online.

Acknowledgements

We thank Ron DePinho for the LKB1$^{fl/fl}$ mice, and Peter J. Mohler for supplying $Na_V1.5$ antibody. We express our thanks to Fred Sigworth and Youshan Yang, for their help and guidance with recording inward sodium currents.

Conflict of interest: none declared.

Funding

This research was supported by NIH grants HL63811 (L.H.Y.), HL097108 (F.G.A.), and T32 HL007950 (V.G.Z.).

References

1. Chugh SS, Havmoeller R, Narayanan K, Singh D, Rienstra M, Benjamin EJ, Gillum RF, Kim YH, McAnulty JH Jr, Zheng ZJ, Forouzanfar MH, Naghavi M, Mensah GA, Ezzati M, Murray CJ. Worldwide epidemiology of atrial fibrillation: a global burden of disease 2010 study. *Circulation* 2014;**129**:837–847.
2. Albarado-Ibanez A, Avelino-Cruz JE, Velasco M, Torres-Jacome J, Hiriart M. Metabolic syndrome remodels electrical activity of the sinoatrial node and produces arrhythmias in rats. *PLoS ONE* 2013;**8**:e76534.
3. Harada M, Nattel SN, Nattel S. Amp-activated protein kinase: potential role in cardiac electrophysiology and arrhythmias. *Circ Arrhythm Electrophysiol* 2012;**5**:860–867.
4. Zaha VG, Young LH. AMP-activated protein kinase regulation and biological actions in the heart. *Circ Res* 2012;**111**:800–814.
5. Lizcano JM, Göransson O, Toth R, Deak M, Morrice NA, Boudeau J, Hawley SA, Udd L, Mäkelä TP, Hardie DG, Alessi DR. LKB1 is a master kinase that activates 13 kinases of the AMPK subfamily, including MARK/PAR-1. *EMBO J* 2004;**23**:833–843.
6. Sakamoto K, Zarrinpashneh E, Budas GR, Pouleur AC, Dutta A, Prescott AR, Vanoverschelde JL, Ashworth A, Jovanović A, Alessi DR, Bertrand L. Deficiency of LKB1 in heart prevents ischemia-mediated activation of AMPKalpha2 but not AMPKalpha1. *Am J Physiol Endocrinol Metab* 2006;**290**:E780–e788.
7. Conde E, Suarez-Gauthier A, Garcia-Garcia E, Lopez-Rios F, Lopez-Encuentra A, Garcia-Lujan R, Morente M, Sanchez-Verde L, Sanchez-Cespedes M. Specific pattern of LKB1 and phospho-acetyl-CoA carboxylase protein immunostaining in human normal tissues and lung carcinomas. *Hum Pathol* 2007;**38**:1351–1360.
8. Baas AF, Boudeau J, Sapkota GP, Smit L, Medema R, Morrice NA, Alessi DR, Clevers HC. Activation of the tumour suppressor kinase LKB1 by the STE20-like pseudokinase STRAD. *EMBO J* 2003;**22**:3062–3072.
9. Boudeau J, Baas AF, Deak M, Morrice NA, Kieloch A, Schutkowski M, Prescott AR, Clevers HC, Alessi DR. MO25alpha/beta interact with STRADalpha/beta enhancing their ability to bind, activate and localize LKB1 in the cytoplasm. *EMBO J* 2003;**22**: 5102–5114.
10. Matsumoto S, Iwakawa R, Takahashi K, Kohno T, Nakanishi Y, Matsuno Y, Suzuki K, Nakamoto M, Shimizu E, Minna JD, Yokota J. Prevalence and specificity of LKB1 genetic alterations in lung cancers. *Oncogene* 2007;**26**:5911–5918.
11. Hemminki A, Markie D, Tomlinson I, Avizienyte E, Roth S, Loukola A, Bignell G, Warren W, Aminoff M, Höglund P, Järvinen H, Kristo P, Pelin K, Ridanpää M, Salovaara R, Toro T, Bodmer W, Olschwang S, Olsen AS, Stratton MR, de la Chapelle A, Aaltonen LA. A serine/threonine kinase gene defective in Peutz-Jeghers syndrome. *Nature* 1998;**391**:184–187.
12. Orlova KA, Parker WE, Heuer GG, Tsai V, Yoon J, Baybis M, Fenning RS, Strauss K, Crino PB. Stradalpha deficiency results in aberrant mTORC1 signaling during corticogenesis in humans and mice. *J Clin Invest* 2010;**120**:1591–1602.
13. Puffenberger EG, Strauss KA, Ramsey KE, Craig DW, Stephan DA, Robinson DL, Hendrickson CL, Gottlieb S, Ramsay DA, Siu VM, Heuer GG, Crino PB, Morton DH. Polyhydramnios, megalencephaly and symptomatic epilepsy caused by a homozygous 7-kilobase deletion in LYK5. *Brain* 2007;**130**:1929–1941.
14. Ylikorkala A, Rossi DJ, Korsisaari N, Luukko K, Alitalo K, Henkemeyer M, Mäkelä TP. Vascular abnormalities and deregulation of VEGF in LKB1-deficient mice. *Science* 2001;**293**:1323–1326.
15. Ollila S, Mäkelä TP. The tumor suppressor kinase LKB1: lessons from mouse models. *J Mol Cell Biol* 2011;**3**:330–340.
16. Thomson DM, Porter BB, Tall JH, Kim HJ, Barrow JR, Winder WW. Skeletal muscle and heart LKB1 deficiency causes decreased voluntary running and reduced muscle mitochondrial marker enzyme expression in mice. *Am J Physiol Endocrinol Metab* 2007;**292**: E196–E202.
17. Thomson DM, Hancock CR, Evanson BG, Kenney SG, Malan BB, Mongillo AD, Brown JD, Hepworth S, Fillmore N, Parcell AC, Kooyman DL, Winder WW. Skeletal muscle dysfunction in muscle-specific LKB1 knockout mice. *J Appl Physiol* 2010;**108**: 1775–1785.
18. Ikeda Y, Sato K, Pimentel DR, Sam F, Shaw RJ, Dyck JR, Walsh K. Cardiac-specific deletion of LKB1 leads to hypertrophy and dysfunction. *J Biol Chem* 2009;**284**: 35839–35849.
19. Bardeesy N, Sinha M, Hezel AF, Signoretti S, Hathaway NA, Sharpless NE, Loda M, Carrasco DR, DePinho RA. Loss of the LKB1 tumour suppressor provokes intestinal polyposis but resistance to transformation. *Nature* 2002;**419**:162–167.
20. Agah R, Frenkel PA, French BA, Michael LH, Overbeek PA, Schneider MD. Gene recombination in postmitotic cells. Targeted expression of Cre recombinase provokes cardiac-restricted, site-specific rearrangement in adult ventricular muscle in vivo. *J Clin Invest* 1997;**100**:169–179.
21. Russell RR, Li J, Coven D, Pypaert M, Zechner C, Palmeri M, Giordano F, Mu J, Birnbaum M, Young L. Amp-activated protein kinase mediates ischemic glucose uptake and prevents postischemic cardiac dysfunction, apoptosis, and injury. *J Clin Invest* 2004; **114**:495–503.
22. Glukhov AV, Fedorov VV, Anderson ME, Mohler PJ, Efimov IR. Functional anatomy of the murine sinus node: high-resolution optical mapping of ankyrin-B heterozygous mice. *Am J Physiol Heart Circ Physiol* 2010;**299**:H482–H491.
23. Akar FG, Nass RD, Hahn S, Cingolani E, Shah M, Hesketh GG, DiSilvestre D, Tunin RS, Kass DA, Tomaselli GF. Dynamic changes in conduction velocity and gap junction properties during development of pacing-induced heart failure. *Am J Physiol Heart Circ Physiol* 2007;**293**:H1223–H1230.
24. Kim AS, Miller EJ, Wright TM, Li J, Qi D, Atsina K, Zaha V, Sakamoto K, Young LH. A small molecule AMPK activator protects the heart against ischemia-reperfusion injury. *J Mol Cell Cardiol* 2011;**51**:24–32.
25. Ehler E, Moore-Morris T, Lange S. Isolation and culture of neonatal mouse cardiomyocytes. *J Vis Exp* 2013; doi: 10.3791/50154.
26. Makara MA, Curran J, Little SC, Musa H, Polina I, Smith SA, Wright PJ, Unudurthi SD, Snyder J, Bennett V, Hund TJ, Mohler PJ. Ankyrin-G coordinates intercalated disc signaling platform to regulate cardiac excitability in vivo. *Circ Res* 2014;**115**:929–938.
27. Qi D, Hu X, Wu X, Merk M, Leng L, Bucala R, Young L. Cardiac macrophage migration inhibitory factor inhibits JNK pathway activation and injury during ischemia/reperfusion. *J Clin Invest* 2009;**119**:3807–3816.
28. Jessen N, Koh HJ, Folmes CD, Wagg C, Fujii N, Løfgren B, Wolf CM, Berul CI, Hirshman MF, Lopaschuk GD, Goodyear LJ. Ablation of LKB1 in the heart leads to energy deprivation and impaired cardiac function. *Biochim Biophys Acta* 2010;**1802**: 593–600.
29. Nattel S, Burstein B, Dobrev D. Atrial remodeling and atrial fibrillation: mechanisms and implications. *Circ Arrhythm Electrophysiol* 2008;**1**:62–73.
30. Whittaker P, Kloner RA, Boughner DR, Pickering JG. Quantitative assessment of myocardial collagen with picrosirius red staining and circularly polarized light. *Basic Res Cardiol* 1994;**89**:397–410.
31. Pytkowski M, Jankowska A, Maciag A, Kowalik I, Sterlinski M, Szwed H, Saumarez RC. Paroxysmal atrial fibrillation is associated with increased intra-atrial conduction delay. *Europace* 2008;**10**:1415–1420.
32. Kongsuphol P, Hieke B, Ousingsawat J, Almaca J, Viollet B, Schreiber R, Kunzelmann K. Regulation of Cl(−) secretion by AMPK in vivo. *Pflugers Arch* 2009;**457**:1071–1078.
33. Andersen RO, Turnbull DW, Johnson EA, Doe CQ. Sgt1 acts via an LKB1/AMPK pathway to establish cortical polarity in larval neuroblasts. *Dev Biol* 2012;**363**:258–265.
34. Delorme B, Dahl E, Jarry-Guichard T, Briand JP, Willecke K, Gros D, Théveniau-Ruissy M. Expression pattern of connexin gene products at the early developmental stages of the mouse cardiovascular system. *Circ Res* 1997;**81**:423–437.
35. Goodenough DA, Goliger JA, Paul DL. Connexins, connexons, and intercellular communication. *Annu Rev Biochem* 1996;**65**:475–502.
36. Kirchhoff S, Nelles E, Hagendorff A, Krüger O, Traub O, Willecke K. Reduced cardiac conduction velocity and predisposition to arrhythmias in connexin40-deficient mice. *Curr Biol* 1998;**8**:299–302.
37. Simon AM, Goodenough DA, Paul DL. Mice lacking connexin40 have cardiac conduction abnormalities characteristic of atrioventricular block and bundle branch block. *Curr Biol* 1998;**8**:295–298.
38. Lei M, Goddard C, Liu J, Léoni AL, Royer A, Fung SS, Xiao G, Ma A, Zhang H, Charpentier F, Vandenberg JI, Colledge WH, Grace AA, Huang CL. Sinus node dysfunction following targeted disruption of the murine cardiac sodium channel gene Scn5a. *J Physiol* 2005;**567**:387–400.
39. Papadatos GA, Wallerstein PM, Head CE, Ratcliff R, Brady PA, Benndorf K, Saumarez RC, Trezise AE, Huang CL, Vandenberg JI, Colledge WH, Grace AA. Slowed conduction and ventricular tachycardia after targeted disruption of the cardiac sodium channel gene Scn5a. *Proc Natl Acad Sci USA* 2002;**99**:6210–6215.
40. Lubkemeier I, Andrie R, Lickfett L, Bosen F, Stockigt F, Dobrowolski R, Draffehn AM, Fregeac J, Schultze JL, Bukauskas FF, Schrickel JW, Willecke K. The connexin40a96s mutation from a patient with atrial fibrillation causes decreased atrial conduction velocities and sustained episodes of induced atrial fibrillation in mice. *J Mol Cell Cardiol* 2013;**65**: 19–32.
41. Jansen JA, Noorman M, Musa H, Stein M, de Jong S, van der Nagel R, Hund TJ, Mohler PJ, Vos MA, van Veen TA, de Bakker JM, Delmar M, van Rijen HV. Reduced heterogeneous expression of Cx43 results in decreased Na_v1.5 expression and reduced sodium current that accounts for arrhythmia vulnerability in conditional Cx43 knockout mice. *Heart Rhythm* 2012;**9**:600–607.
42. Gaborit N, Steenman M, Lamirault G, Le Meur N, Le Bouter S, Lande G, Leger J, Charpentier F, Christ T, Dobrev D, Escande D, Nattel S, Demolombe S. Human atrial ion channel and transporter subunit gene-expression remodeling associated with valvular heart disease and atrial fibrillation. *Circulation* 2005;**112**:471–481.
43. Ozcan C, Battaglia E, Young R, Suzuki G. LKB1 knockout mouse develops spontaneous atrial fibrillation and provides mechanistic insights into human disease process. *J Am Heart Assoc* 2015;**4**:e001733.
44. Tanaka K, Zlochiver S, Vikstrom KL, Yamazaki M, Moreno J, Klos M, Zaitsev AV, Vaidyanathan R, Auerbach DS, Landas S, Guiraudon G, Jalife J, Berenfeld O, Kalifa J. Spatial distribution of fibrosis governs fibrillation wave dynamics in the posterior left atrium during heart failure. *Circ Res* 2007;**101**:839–847.

45. Nakajima H, Nakajima HO, Salcher O, Dittiè AS, Dembowsky K, Jing S, Field LJ. Atrial but not ventricular fibrosis in mice expressing a mutant transforming growth factor-beta(1) transgene in the heart. *Circ Res* 2000;**86**:571–579.
46. Akar FG, Spragg DD, Tunin RS, Kass DA, Tomaselli GF. Mechanisms underlying conduction slowing and arrhythmogenesis in nonischemic dilated cardiomyopathy. *Circ Res* 2004;**95**:717–725.
47. Sung MM, Zordoky BN, Bujak AL, Lally JS, Fung D, Young ME, Horman S, Miller EJ, Light PE, Kemp BE, Steinberg GR, Dyck JR. AMPK deficiency in cardiac muscle results in dilated cardiomyopathy in the absence of changes in energy metabolism. *Cardiovasc Res* 2015;**107**:235–245.
48. Quentin T, Kitz J, Steinmetz M, Poppe A, Bar K, Kratzner R. Different expression of the catalytic alpha subunits of the amp activated protein kinase—an immunohistochemical study in human tissue. *Histol Histopathol* 2011;**26**:589–596.
49. Gollob MH, Green MS, Tang AS, Gollob T, Karibe A, Ali Hassan AS, Ahmad F, Lozado R, Shah G, Fananapazir L, Bachinski LL, Roberts R. Identification of a gene responsible for familial Wolff-Parkinson-White syndrome. *N Engl J Med* 2001;**344**:1823–1831.
50. Arad M, Moskowitz IP, Patel VV, Ahmad F, Perez-Atayde AR, Sawyer DB, Walter M, Li GH, Burgon PG, Maguire CT, Stapleton D, Schmitt JP, Guo XX, Pizard A, Kupershmidt S, Roden DM, Berul CI, Seidman CE, Seidman JG. Transgenic mice overexpressing mutant PRKAG2 define the cause of Wolff-Parkinson-White syndrome in glycogen storage cardiomyopathy. *Circulation* 2003;**107**:2850–2856.
51. Wirka RC, Gore S, Van Wagoner DR, Arking DE, Lubitz SA, Lunetta KL, Benjamin EJ, Alonso A, Ellinor PT, Barnard J, Chung MK, Smith JD. A common connexin-40 gene promoter variant affects connexin-40 expression in human atria and is associated with atrial fibrillation. *Circ Arrhythm Electrophysiol* 2011;**4**:87–93.
52. Chen LY, Ballew JD, Herron KJ, Rodeheffer RJ, Olson TM. A common polymorphism in Scn5a is associated with lone atrial fibrillation. *Clin Pharmacol Ther* 2007;**81**:35–41.
53. Ellinor PT, Nam EG, Shea MA, Milan DJ, Ruskin JN, MacRae CA. Cardiac sodium channel mutation in atrial fibrillation. *Heart Rhythm* 2008;**5**:99–105.
54. Olesen MS, Yuan L, Liang B, Holst AG, Nielsen N, Nielsen JB, Hedley PL, Christiansen M, Olesen SP, Haunso S, Schmitt N, Jespersen T, Svendsen JH. High prevalence of long QT syndrome-associated Scn5a variants in patients with early-onset lone atrial fibrillation. *Circulation* 2012;**5**:450–459.